Hydrogen and muonium in diamond: A path-integral molecular dynamics simulation

Carlos P. Herrero and Rafael Ramírez
Instituto de Ciencia de Materiales, Consejo Superior de Investigaciones Científicas (CSIC), Campus de Cantoblanco, 28049 Madrid, Spain

Eduardo R. Hernández
Institut de Ciència de Materials de Barcelona (ICMAB), Consejo Superior de Investigaciones Científicas (CSIC), Campus de Bellaterra, 08193 Barcelona, Spain

(Dated: February 6, 2008)

Isolated hydrogen, deuterium, and muonium in diamond have been studied by path-integral molecular dynamics simulations in the canonical ensemble. Finite-temperature properties of these point defects were analyzed in the range from 100 to 800 K. Interatomic interactions were modeled by a tight-binding potential fitted to density-functional calculations. The most stable position for these hydrogenic impurities is found at the C–C bond center. Vibrational frequencies have been obtained from a linear-response approach, based on correlations of atom displacements at finite temperatures. The results show a large anharmonic effect in impurity vibrations at the bond center site, which hardens the vibrational modes with respect to a harmonic approximation. Zero-point motion causes an appreciable shift of the defect level in the electronic gap, as a consequence of electron-phonon interaction. This defect level goes down by 70 meV when replacing hydrogen by muonium.

PACS numbers: 61.72.-y, 71.55.Cn, 81.05.Uw

I. INTRODUCTION

In spite of being one of the simplest possible impurities, a detailed understanding of the physical properties of isolated hydrogen in group-IV materials requires the combination of advanced experimental and theoretical methods.[1,2] Experimental investigations on atomic, interstitial hydrogen have been so far scarce, since H has turned out to be difficult to observe as an isolated impurity in these materials. In silicon, electron paramagnetic resonance experiments[3,4] indicated that hydrogen is located at a bond-center (BC) site, midway between two nearest-neighbor host atoms, in agreement with several theoretical calculations.[2,5] However, for isolated hydrogen in diamond there is little detailed experimental information available in the literature. In this context, muonium may be considered as a light pseudoisotope of hydrogen, due to the small mass of the muon μ^+ (about 1/9 that of the proton). This means that in many respects muonium is expected to behave similarly to hydrogen, with the appropriate corrections due to zero-point motion and related effects. Thus, muon implantation experiments in diamond as well as several theoretical approaches have shown that this impurity is metastable at a tetrahedral interstitial site (the so-called 'normal muonium'), and has its lowest energy at or around the bond center site ('anomalous muonium').[2,6,7]

Apart from its basic interest as an isolated impurity, an important property of hydrogen in solids is its ability to form complexes and passivate defects. This has been extensively studied in the last twenty years for silicon and germanium.[1,2] More recently, it has been noted that hydrogen can also passivate impurities in diamond.[8,9] Over the last years, there has been an intense theoretical activity on hydrogen-related defects in this material.[10,11,12,13] For isolated hydrogen in the neutral charge state, most of the calculations found the BC site as the lowest-energy position for this impurity in diamond. Some deviations from the BC site were found by Saada *et al.*[14] from a tight-binding (TB) calculation. Also, for hydrogen in the positive charge state, density-functional theory calculations have found this impurity to be stable off-axis in a buckled bond-centered configuration.[15,16]

In standard electronic-structure calculations in condensed matter, despite of their quantum mechanical character, atomic nuclei are treated as classical particles, and therefore typical quantum effects like zero-point vibrations are not directly accessible. These quantum effects can be important for vibrational and electronic properties of light impurities like hydrogen, especially at low temperatures. In fact, the importance of taking into account the quantum character of proton and muon to study hydrogen-related point defects in diamond has been emphasized by Kerridge *et al.*[17] In particular, quantum tunneling is relevant to understand the properties of vacancy-hydrogen complexes in this material.[18]

Finite-temperature properties of hydrogen-related defects in solids have been studied by *ab initio* and tight-binding molecular dynamics (MD) simulations. In many previous applications of these methods, the atomic nuclei were treated as classical particles.[19,20,21] In order to consider the quantum nature of the nuclei, the path-integral molecular dynamics (or Monte Carlo) approach has proved to be very useful. A remarkable advantage of this method is that all nuclear degrees of freedom can be quantized in an efficient manner, thus permitting the inclusion of both quantum and thermal fluctuations in many-body systems at finite temperatures. In this way, Monte Carlo or molecular dynamics sampling applied to evaluate finite-temperature path integrals allows one to

carry out quantitative and nonperturbative studies of highly-anharmonic effects in solids.[22,23]

In this paper, the path-integral molecular dynamics (PIMD) method is used to investigate the role of the impurity mass on the properties of hydrogenic point defects. We consider isolated hydrogen, deuterium (D) and muonium (Mu) in diamond, in their neutral charge state. Special attention has been paid to the vibrational properties of these impurities, by considering anharmonic effects on their quantum dynamics. The results of the present calculations show that such anharmonic effects lead to a significant deviation of the vibrational frequencies of the impurities, as compared to a harmonic approximation. Also, zero-point motion causes an appreciable shift of the defect levels in the electronic gap, which is a manifestation of the electron-phonon interaction induced by the hydrogenic impurities. Path-integral methods analogous to that employed in this work have been applied earlier to study hydrogen in metals[22,24] and semiconductors.[25,26,27]

The paper is organized as follows. In Sec. II, we describe the computational method and the models employed in our calculations. Our results are presented in Sec. III, dealing with the energy of the defects, vibrational frequencies, and defect levels in the electronic gap of diamond. Sec. IV includes a discussion of the results and a summary.

II. COMPUTATIONAL METHOD

A. Path-integral molecular dynamics

In the path-integral formulation of statistical mechanics, the partition function is evaluated through a discretization of the density matrix along cyclic paths, composed of a finite number L (Trotter number) of "imaginary-time" steps.[28,29] In the numerical simulations, this discretization gives rise to the appearance of L "beads" for each quantum particle. Thus, this method exploits the fact that the partition function of a quantum system is formally equivalent to that of a classical one, obtained by replacing each quantum particle by a ring polymer consisting of L particles, connected by harmonic springs.[22,23] In many-body problems, the configuration space is usually sampled by Monte Carlo or molecular dynamics techniques. Here, we have employed the PIMD method, which has been found to require less computer time resources in our problem. Effective algorithms to perform PIMD simulations in the canonical NVT ensemble have been described in detail by Martyna *et al.*[30] and Tuckerman.[31] All calculations presented here were carried out in the canonical ensemble, using an originally developed MD software, which enables efficient PIMD simulations on parallel supercomputers.

The calculations have been performed within the adiabatic (Born-Oppenheimer) approximation, which allows us to define a potential energy surface for the nuclear coordinates. As in classical molecular dynamics simulations, an important issue of the PIMD method is the proper description of interatomic interactions, which should be as realistic as possible. To overcome the limitations of effective classical potentials to reproduce the many-body energy surface, one has to resort to self-consistent quantum-mechanical methods. Nevertheless, true density functional or Hartree-Fock based self-consistent potentials require computer resources that would restrict enormously the size of our simulation cell. We have found a reasonable compromise by deriving the Born-Oppenheimer surface for the nuclear dynamics from an efficient tight-binding effective Hamiltonian, based on density functional (DF) calculations.[32] The capability of tight-binding methods to simulate different properties of solids and molecules has been reviewed by Goringe *et al.*[33] We have checked the ability of this DF-TB potential to predict frequencies of C–H vibrations. In particular, for a methane molecule it predicts in a harmonic approximation frequencies of 3100 and 3242 cm^{-1} for C–H modes with symmetry A_1 and T_2, respectively, to be compared with experimental frequencies of 2917 and 3019 cm^{-1}.[34] Taking into account the typical anharmonic shift associated to these modes (towards lower frequencies), the agreement is satisfactory. A detailed analysis of vibrational frequencies of hydrocarbon molecules derived with the present DF-TB potential, including anharmonicities, can be found elsewhere.[35,36]

Simulations were carried out on a $2 \times 2 \times 2$ supercell of the diamond face-centered cubic cell with periodic boundary conditions, containing 64 C atoms and one impurity. For comparison, we also carried out simulations of diamond without impurities, using the same supercell size. In our calculations, four symmetry independent k points in the Brillouin zone of the simulation supercell were employed, distributed by following the Monkhorst-Pack generation scheme.[37] We have checked the convergence of the internal energy for some selected atom configurations, by considering up to 32 k points. In particular, the internal energy of hydrogen on the tetrahedral T site and on the BC configuration changes by about 1 meV, respect to our calculation employing 4 k points. Sampling of the configuration space has been carried out at temperatures between 100 and 800 K. The simulation-cell parameter employed in our calculations was taken from experimental data[38] and thus changed from 7.1336 Å at 100 K to 7.1424 Å at 800 K. For a given temperature, a typical run consisted of 10^4 MD steps for system equilibration, followed by 10^5 steps for the calculation of ensemble average properties.

To have a nearly constant precision in the path integral results at different temperatures, we have taken a Trotter number that scales as the inverse temperature. At 300 K we took $L = 20$ for H and D, and $L = 70$ for Mu. For comparison with the results of our PIMD simulations, we have carried out some classical MD simulations with the same interatomic interaction (setting $L = 1$). Note that for equilibrium properties in the canonical ensemble (i.e., mean energy, spatial distribution), the

classical limit is equivalent in our context to the infinite-mass limit ($m \to \infty$). The quantum simulations were performed using a staging transformation for the bead coordinates. Chains of four Nosé-Hoover thermostats with mass $Q = \beta\hbar^2/5L$ were coupled to each degree of freedom to generate the canonical ensemble.[39] To integrate the equations of motion, we have used the reversible reference system propagator algorithm (RESPA), which allows one to define different time steps for the integration of the fast and slow degrees of freedom.[30] The time step Δt associated to the calculation of DF-TB forces was taken in the range between 0.2 and 0.5 fs, which was found to be appropriate for the interactions, atomic masses, and temperatures considered here. For the evolution of the fast dynamical variables, that include the thermostats and harmonic bead interactions, we used a smaller time step $\delta t = \Delta t/4$. We note that for muonium at 200 K (the lowest temperature considered for this impurity), a simulation run of 10^5 MD steps requires the calculation of forces and energy with the tight-binding code for about 10^7 configurations, which needs the use of large parallel computers.

B. Calculation of anharmonic vibrational frequencies

Important characteristics of impurities in solids are their vibrational frequencies, which are known to be dependent on the particular site occupied by a given impurity in the crystal and on its interactions with the nearby hosts atoms. In our context, the question arises whether the oscillator frequencies associated to an impurity located at a given site can be extracted by assuming the host C atoms fixed in the relaxed geometry. This is in fact a method frequently employed to calculate vibrational frequencies of impurities in solids. On the other side, when all C atoms are allowed to relax by following the impurity motion, the potential energy surface is much flatter (smaller energy changes) than when the host atoms are fixed. To obtain an approach for the actual vibrational frequencies of the impurities, one can calculate the eigenvalues of the dynamical matrix of the whole simulation cell, and obtain the frequencies in the harmonic approximation (HA). However, for light impurities and atomic configurations displaying large strains (important relaxations), the anharmonicity can be appreciable, making the harmonic frequencies meaningless.

To calculate these anharmonic frequencies we will employ a method based on the linear response (LR) of the system to vanishingly small forces applied on the atomic nuclei. With this purpose, we consider a LR function, the static isothermal susceptibility χ^T, that is readily derived from PIMD simulations of the equilibrium solid, without dealing explicitly with any external forces in the simulation. This approach represents a significant improvement as compared to a standard harmonic approximation.[40] A sketch of the method is given in the following.

Let us call $\{x_{ip}\}$ the set of $3NL$ Cartesian coordinates of the beads forming the ring polymers in the simulation cell ($i = 1, \ldots, 3N; p = 1, \ldots, L$). We consider the set $\{X_i\}$ of centroid coordinates, with X_i defined as the mean value of coordinate i over the corresponding polymer:

$$X_i = \frac{1}{L}\sum_{p=1}^{L} x_{ip} \ . \tag{1}$$

Then, the linear response of the quantum system to small external forces on the atomic nuclei is given by the susceptibility tensor χ^T, that can be defined in terms of centroid coordinates as[40]

$$\chi^T_{ij} = \beta\sqrt{m_i m_j}\ \mu_{ij} \ , \tag{2}$$

where $\beta = (k_B T)^{-1}$, m_i is the mass of the nucleus associated to coordinate i, $\mu_{ij} = \langle X_i X_j\rangle - \langle X_i\rangle\langle X_j\rangle$ is the covariance of the centroid coordinates X_i and X_j, and $\langle \ldots \rangle$ indicates an ensemble average along a MD run.

The tensor χ^T allows us to derive a LR approximation to the low-lying excitation energies of the vibrational system, that is applicable even to highly anharmonic situations. The LR approximation for the vibrational frequencies reads

$$\omega_{n,LR} = \frac{1}{\sqrt{\Delta_n}} \ , \tag{3}$$

where Δ_n ($n = 1, \ldots, 3N$) are eigenvalues of χ^T, and the LR approximation to the low-lying excitation energy of vibrational mode n is given by $\hbar\omega_{n,LR}$. More details on the method and illustrations of its ability for predicting vibrational frequencies of solids and molecules can be found elsewhere.[35,40,41,42] In connection with the vibrational modes that actually appear in our calculations, we note that the application of periodic boundary conditions is physically equivalent to the only consideration of lattice vibrations at the center ($k = 0$) of the Brillouin zone of the simulation cell.[42]

III. RESULTS

A. Energy

We first discuss the stable sites for the hydrogenic impurities in diamond, as derived from classical calculations at $T = 0$, i.e., point nuclei without spatial delocalization. In this respect, Estle *et al.*[7] noticed the importance of lattice relaxation for finding the most stable site for the impurities, and obtained that interstitial bond-centered hydrogen or muonium is stable as a result of unusually large lattice relaxation. This is in fact the case for the DF-TB model employed here. After relaxation of the host atoms, the energy surface has minima only at two non-equivalent positions. The lowest-energy position is

the BC site, as in several earlier investigations.[15] In the relaxed configuration, we find a distance C–H of 1.17 Å, which means a backward relaxation of the adjacent C atoms of 0.40 Å. This indicates that the formation of the C–H–C bridge requires a large dilation of the C–C bond (a 52% of the original one). These values agree with those found earlier from tight-binding calculations of hydrogen in diamond.[14,43]

Another local minimum of the energy surface is found for the impurity at the tetrahedral T site, located 1.44 eV above the absolute minimum. In this configuration, the relaxation of the nearest lattice atoms is much smaller than for the bond-center configuration (0.08 Å). There appears in the literature a rather large dispersion of values for the relative energy of H on the T site. These values range typically from 0.5 to 2.7 eV.[15] Then, our result lies in the intermediate region of these earlier values, and in particular it is close to that reported by Kaukonen *et al.*[43] from a DF-TB calculation (1.6 eV). For the energy barrier from a BC to a T site we find 1.7 eV, a value between those obtained from local-density functional theory[16] (1.6 eV) and earlier DF-TB calculations[43] (2.0 ± 0.1 eV). For the migration barrier from T to BC sites we have found 0.3 eV, to be compared with 0.4 ± 0.1 eV obtained in Ref. 43. We note that the so-called antibonding site, between an atom and a T site along a $\langle 111 \rangle$ direction, has turned out to be from our TB calculations a saddle point on the energy surface, contrary to Ref. 43, where a local minimum was reported.

We now turn to our simulations at finite temperatures. The internal energy, $E(V,T)$, at volume V and temperature T can be written as:

$$E(V,T) = E_{\rm min}(V) + E_{\rm v}(V,T)\,, \qquad (4)$$

where $E_{\rm min}(V)$ is the potential energy for the classical solid at $T = 0$, and $E_{\rm v}(V,T)$ is the vibrational energy. At finite temperatures, V changes with T due to thermal expansion. The vibrational energy, $E_{\rm v}(V,T)$, depends explicitly on both V and T, and can be obtained by subtracting the energy $E_{\rm min}(V)$ from the internal energy. In this way, path-integral molecular dynamics simulations allow us to obtain $E_{\rm v}(V,T)$ for a given volume and temperature.

Shown in Fig. 1 is the temperature dependence of the vibrational energy $E_{\rm v}$ per simulation cell for hydrogenic impurities at the BC site. Symbols indicate results of PIMD simulations: deuterium (circles), hydrogen (squares), and muonium (triangles). For comparison we also show $E_{\rm v}$ for pure diamond (triangles). At 300 K, the vibrational energy of diamond amounts to 12.4 eV per simulation cell, i.e., 0.19 eV/atom. As expected, $E_{\rm v}$ increases as temperature is raised, and eventually converges to the classical limit $E_{\rm v}^{cl} = 3Nk_BT$ at high T. When we consider the hydrogenic impurities at the BC site, the vibrational energy increases as compared to pure diamond. This increase is larger the lower the impurity mass, as a consequence of zero-point motion.

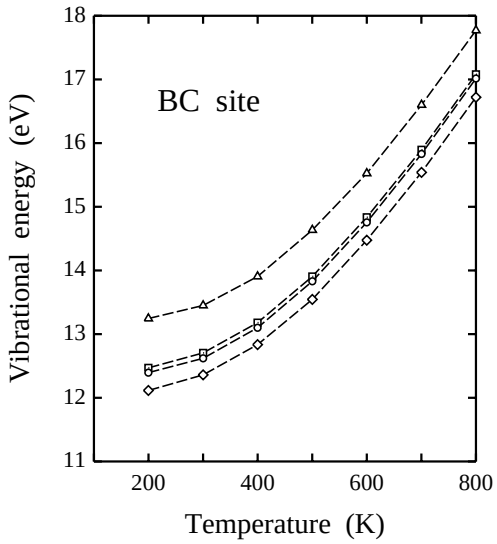

FIG. 1: Temperature dependence of the vibrational energy of the $2 \times 2 \times 2$ diamond supercell with one impurity, as derived from PIMD simulations. Results are shown for deuterium (circles), hydrogen (squares), and muonium (triangles). For comparison, we also present results for a pure diamond supercell (diamonds). Dashed lines are guides to the eye. Error bars are less than the symbol size.

At this point, an interesting characteristic of the different hydrogenic defects is their associated vibrational energy. At a given temperature, this energy is defined as the difference $\Delta E_{\rm v} = E_{\rm v}(64{\rm C} + {\rm Imp}) - E_{\rm v}(64{\rm C})$, where 'Imp' stands for H, D, or muonium. Note that $\Delta E_{\rm v}$ so defined is not just the vibrational energy of a given impurity in the crystal, but it also includes changes in the vibrations of the host atoms. In Fig. 2, the energy $\Delta E_{\rm v}$ is plotted vs temperature for the considered impurities at a BC site. Within the numerical precision of our MD simulations, $\Delta E_{\rm v}$ turns out to be constant for the three hydrogenic impurities. This means that at temperatures lower than 800 K we find for these defects, $\Delta E_{\rm v}$ values basically the same as their corresponding zero-temperature limit. A slight increase of this energy should be expected in the temperature region shown in Fig. 2, especially for H and D (with vibrational frequencies lower than for Mu), due to thermal excitation of higher vibrational modes. However, it seems that this increase is compensated for by a decrease due to lattice expansion, with its associated softening of the vibrational modes. In fact, we have carried out a PIMD simulation of H at a BC site with the lattice parameter corresponding to 200 K ($a = 3.5668$ Å), and found $\Delta E_{\rm v} = 0.40$ eV, about 50 meV higher than the value obtained using the actual lattice parameter at 800 K ($a = 3.5712$ Å). For comparison with our results of PIMD, we also show in Fig. 2 results for $\Delta E_{\rm v}$ derived from classical MD simulations (diamonds). These data points follow closely the trend expected for a classical three-dimensional harmonic oscillator: $\Delta E_{\rm v} = 3k_BT$.

TABLE I: Vibrational energy $\Delta E_{\rm v}$ of hydrogenic defects and position of the defect level, E_I, at 300 K for impurities at BC and T sites, as derived from PIMD simulations. Energy is given in eV, and the zero of energy for the electronic levels is taken at the valence-band top. Also given are the ratios between vibrational energies for different impurities. Error bars in $\Delta E_{\rm v}$ are $\pm$ 6 meV for H and D, and $\pm$ 10 meV for Mu. The statistical error for E_I is $\pm$2 meV .

	Vibrational energy		Defect level	
Impurity	BC	T	BC	T
classical	0.071	0.078	2.612	3.193
D	0.260	0.345	2.592	3.280
H	0.347	0.478	2.579	3.326
Mu	0.992	1.439	2.509	3.659
$\Delta E_{\rm v}^D$ / $\Delta E_{\rm v}^H$	0.75	0.72		
$\Delta E_{\rm v}^{Mu}/\Delta E_{\rm v}^H$	2.86	3.01		

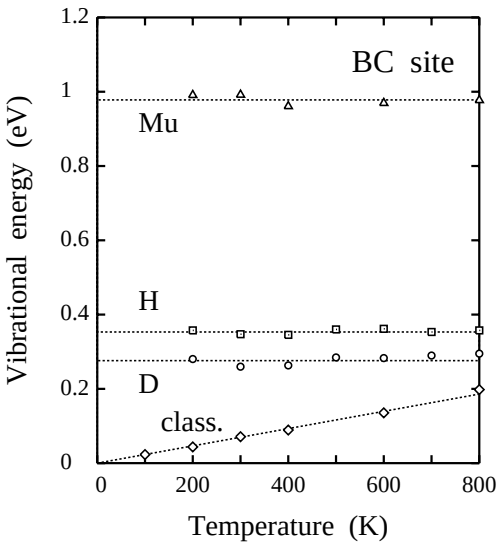

FIG. 2: Vibrational energy of the hydrogenic defects as a function of temperature. Results are shown for deuterium (circles), hydrogen (squares), and muonium (triangles). For comparison, we also present the vibrational energy derived from classical MD simulations. Error bars are on the order of the symbol size. Dotted lines are guides to the eye.

In a one-particle harmonic approximation, the low-temperature vibrational energies corresponding to deuterium, hydrogen, and muonium scale as $0.71 : 1 : 2.97$, i.e., proportional to $m^{-1/2}$ (m, impurity mass). In Table I we give the vibrational energies of the hydrogenic defects and ratios between them. At 300 K, $\Delta E_{\rm v}$ values derived from our PIMD simulations scale as $0.75 : 1 : 2.86$, with ratios somewhat different from those for a harmonic approximation. In fact, we have estimated error bars of ± 0.02 and ± 0.05 for the ratios $\Delta E_{\rm v}^D/\Delta E_{\rm v}^H$ and $\Delta E_{\rm v}^{Mu}/\Delta E_{\rm v}^H$, respectively. This is an indication of the anharmonicity present in the defect vibrations, which will be discussed below.

By using the same procedure, we have calculated the vibrational energy $\Delta E_{\rm v}$ for impurities at the T site. The results at 300 K are given in Table I. The resulting energies are larger than the corresponding ones for the BC configuration. At first sight, this result may seem surprising, taking into account the constrained geometry of the BC configuration, which should give a larger frequency for the stretching vibration along the C–H–C axis. However, vibrations transverse to this axis are expected to have much lower frequency, making reasonable a larger $\Delta E_{\rm v}$ for the T defect with threefold degenerate vibrational modes (see below). For the energy ratios at the T configuration we find $0.72 : 1 : 3.01$, which are compatible within error bars with a harmonic approach.

A detailed analysis of the temperature dependence of properties of the impurities at the T site is not feasible due to the metastability of these defects. The metastability of hydrogen at the T site is illustrated in Fig. 3, where we show the energy of the simulation cell along a PIMD run at 600 K. This simulation run started with H at a T site, and after about 15000 steps we observed the passage of the impurity to a BC site. This is reflected in the figure by an energy jump of about 1.6 eV, which corresponds to the difference between energy minima plus the difference between vibrational energies. Similar results were obtained in other simulations at the same temperature, with hydrogen typically jumping from T to BC positions after a number of MD steps in the range from 10^4 to 10^5. However, at 300 K hydrogen remained around the metastable T site during several simulation runs of 10^5 steps, and the same happened for deuterium and muonium. We remember that the time scale of a simulation run (i.e., Δt times the number of MD steps) does

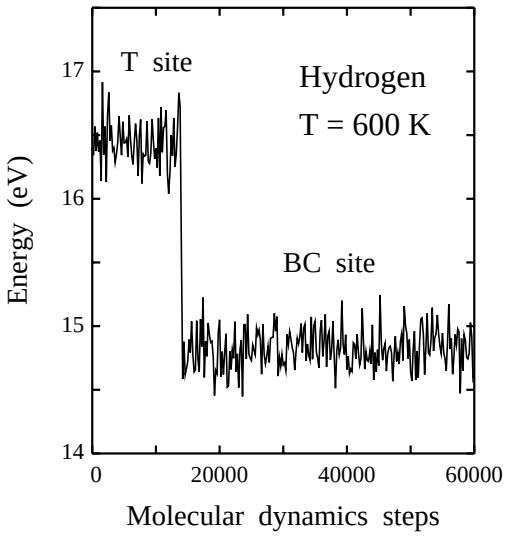

FIG. 3: Internal energy of the simulation cell along a PIMD trajectory at 600 K, starting with hydrogen on a T site. One observes a drop in the energy after about 15000 steps, corresponding to a passage of hydrogen from the T-site region to the BC well. The zero of energy is taken for a classical system with the impurity on a BC site at $T = 0$ (absolute energy minimum).

not represent a real physical time, since the dynamics of the beads in the ring polymers does not correspond to the actual dynamics of the quantum particles. The fictitious bead dynamics is merely used as an efficient way to calculate equilibrium properties of the system in the canonical ensemble. Thus, the plot in Fig. 3 illustrates the ability of PIMD to explore the configuration space, and to drive the system to the most stable region, once the temperature is high enough. For comparison, we note that the metastability of muonium at the T site has been observed by muon spin rotation.[44] In fact, 'isotropic muonium' (at T) converts to 'anisotropic muonium' (at BC) in the range 500–700 K.

B. Vibrational frequencies

As indicated above, the DF-TB potential gives a good description of vibrational modes in hydrocarbon molecules. To check the reliability of this potential to give vibrational frequencies of hydrogenic impurities in diamond, and to assess their anharmonicity, we have carried out calculations for a simple atomic cluster (see Fig. 4). In this cluster, the impurity occupies a position similar to a BC site in the diamond lattice, midway between two carbon atoms with a distance d(C,H) = 1.17 Å, as that found in diamond with the DF-TB potential. In this atomic cluster, we have calculated total energies for hydrogen displacements along the C–C axis, with both our TB Hamiltonian and the B3LYP density-functional

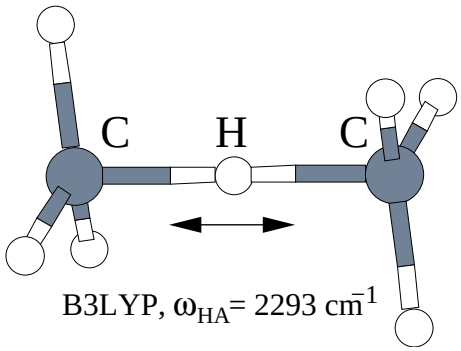

FIG. 4: Schematic representation of the atomic cluster employed to compare total energy changes obtained with our tight-binding approach and with the B3LYP model. ω_{HA} indicates the vibrational frequency for hydrogen along the C–C direction, obtained in a single-particle harmonic approximation in either case.

theory (with the cc-pDVZ basis set as implemented in the Gaussian 98 package).[45] Results obtained by both methods are shown in Fig. 5, where the zero of energy corresponds to the BC position in either case. The continuous and dashed lines correspond to DF-TB and B3LYP models, respectively. The curvature of the solid line at the minimum is smaller than that of the dashed line, and thus the harmonic approach gives for the DF-TB method a vibrational frequency (1991 cm^{-1} for H) lower, but of the same order, than that of the B3LYP potential (2293 cm^{-1} for H). We emphasize that these energy curves do not correspond to hydrogenic impurities in bulk diamond, but they help to analyze the reliability of the DF-TB potential and to illustrate qualitatively the vibrational potential of these impurities in the solid.

In Fig. 5 we also present the two lowest energy levels for hydrogen, obtained by numerically solving the one-dimensional Schrödinger equation with each interaction model. Now the ground state for the B3LYP potential is higher than that of the DF-TB model. The first excited states yielded by both procedures are very close to one another, and in fact are indistinguishable on the scale of Fig. 5. We then find that the excitation energy $\hbar(\omega_1 - \omega_0)$ corresponds to 2633 and 2577 cm^{-1} for DF-TB and B3LYP, respectively. In both cases we find excitation energies larger than in the harmonic approximation, i.e., anharmonicity hardens the stretching vibration, as expected for an impurity in a highly-confined geometry. The excitation energies obtained by both methods are similar, with a relative difference between them smaller than 3%, which gives us confidence in the reliability of the DF-TB method to analyze vibrational properties of hydrogenic point defects in diamond.

We now go back to the study of hydrogenic impurities in bulk diamond. Before analyzing the anharmonic modes given by the linear response procedure described in Sec. II.B, we will present the vibrational frequencies

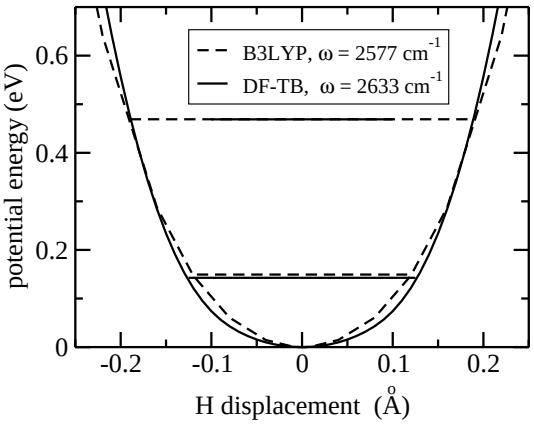

FIG. 5: Potential energy curves for impurity displacements along the direction parallel to the C–C axis, with fixed carbon atoms, in the cluster shown in Fig. 4. The minimum potential energy corresponds to the impurity at the bond-center site. Horizontal lines represent energy levels for hydrogen, obtained by numerically solving the one-dimensional Schrödinger equation with those potentials. Results are shown for the tight-binding potential employed here (solid lines) and for the B3LYP model (dashed lines). The given frequencies correspond to first excitation energies in both cases.

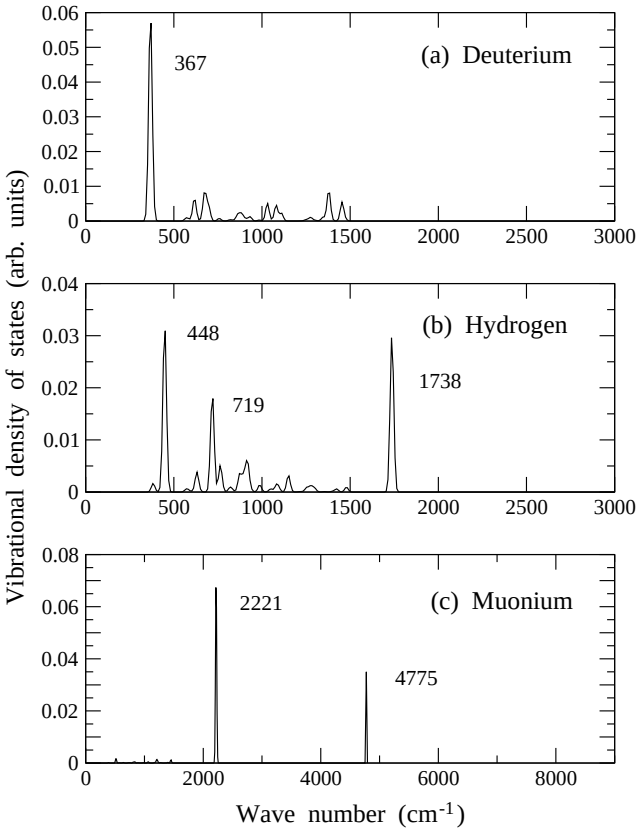

FIG. 6: Vibrational density of states for impurities at a BC site, as derived from the dynamical matrix of the simulation cell in a harmonic approximation. Each panel corresponds to an impurity: (a) deuterium, (b) hydrogen, (c) muonium. Labels indicate wave numbers in cm^{-1}. For the sake of clarity, discrete modes have been broadened to Gaussian profiles with a standard deviation of 10 cm^{-1}. Note the different horizontal scale in panel (c).

of the impurities derived from a harmonic approximation. This will allow us to assess the importance of anharmonicity for the impurity vibrations. By calculating the dynamical matrix, we find the vibrational density of states (VDOS) corresponding to the whole simulation cell (64 C atoms plus one impurity). We then use the amplitude of the displacement of the impurity in each vibrational mode, to obtain its partial VDOS. This is shown in Fig. 6 for (a) deuterium, (b) hydrogen, and (c) muonium at the BC site. The results can be most clearly understood for the case of muonium, where one observes basically two peaks at 2221 and 4775 cm^{-1}, well separated from the region of crystal vibrations (up to about 1500 cm^{-1}). Due to the low mass of Mu, these vibrations are almost totally decoupled from the host-atom vibrations, and are associated to motion perpendicular (bending, twofold degenerate) and parallel (stretching) to the C–C axis, respectively. This is in fact the situation expected for an impurity at a BC site, assuming fixed host atoms. The partial VDOS is, however, more complicated for H and D, which participate in modes that are not totally localized at the impurity atom or at the impurity plus its nearest C neighbors. For H, we find only one mode with frequency larger than the lattice modes, corresponding to the stretching vibration along the C–H–C bond ($\omega_{\parallel,HA} = 1738$ cm^{-1}). We obtain two other peaks at 448 and 719 cm^{-1} with large participation of hydrogen motion. They are assigned to transverse vibrations, perpendicular to the C–H–C axis, and include important participation of nearby C atoms. For deuterium, the most prominent feature is a large peak at 367 cm^{-1}, corresponding to bending vibrations. In this case, the stretching vibration is highly coupled to crystal modes, and does not appear as a prominent peak in the VDOS.

Next, we apply the linear-response procedure to obtain the (anharmonic) vibrational frequencies of the impurities. Again, we obtain the VDOS of the whole simulation cell and project from it the contribution of the considered impurity. This partial VDOS is shown in Fig. 7 for the hydrogenic impurities studied here at 300 K. As before, we first comment on the results for muonium in panel (c). We observe two distinct peaks, as for the HA, but now at much higher frequencies. This resembles the effect of anharmonicity observed for the atomic cluster considered above. For muonium at a BC site in diamond, both vibrations parallel and perpendicular to the C–Mu–C axis harden strongly due to anharmonicity. Something similar happens for hydrogen and deuterium, as noticed when one compares the corresponding panels in Figs. 6 and 7. For hydrogen, an interesting feature is the appearance of a second peak at 1559 cm^{-1}, above but close

to the largest frequency in bulk diamond, corresponding to a bending mode [Fig. 7(b)]. For deuterium, we obtain a well-resolved stretching mode at 1837 cm^{-1}, far in frequency from the lattice vibrations. For the frequencies derived from the LR method, we estimate error bars of 20 cm^{-1}, due to the statistical noise present in the susceptibility tensor χ^T derived from the PIMD simulations. For the different impurities, the highest-frequency mode $\omega_{\parallel,LR}$ scales as 0.72 : 1 : 3.13, to be compared with the ratio 0.71 : 1 : 2.97 expected for one-particle harmonic oscillators. The stretching frequency derived for H from our LR calculations ($\omega_{\parallel,LR}$ = 2544 cm^{-1}) is lower than that obtained for this impurity by Goss *et al.*[15,16] from DF calculations in the harmonic approximation (2919 cm^{-1}). This difference can be explained, at least in part, by the difference in the C–H distance obtained by both methods: 1.17 Å for our TB potential vs 1.13 Å for the DF calculations[16] (the larger the distance, the lower is expected to be this frequency). We also note that DF calculations predict a frequency of 2456 cm^{-1} for positively charged hydrogen in a buckled bond-centered configuration.[16]

We have repeated the same LR procedure to calculate the vibrational frequencies of hydrogenic impurities at the T site. In this case, we find for each impurity a threefold degenerate mode, in agreement with the tetrahedral point symmetry of this site. Coupling with lattice vibrational modes is negligible. We find the frequencies 2088, 2818, and 7284 cm^{-1} for D, H, and Mu, respectively, which translates to a frequency ratio 0.74:1:2.58. For impurities at the T site, anharmonicity causes a softening of the modes. For example, for hydrogen we find in the HA a frequency of 3099 cm^{-1}, more than 200 cm^{-1} larger than that found with the LR method. This softening is still more important for muonium, due to its larger zero-point vibration, and is the origin of the small ratio $\omega^{Mu}_{||,LR}/\omega^{H}_{||,LR} = 2.58$ (to be compared with a ratio of 2.97 expected for harmonic oscillators). We note that anharmonicity affects the mode frequencies in opposite ways at the BC and T sites. While the vibrational modes associated to the impurities at the BC site suffer a strong shift towards higher frequencies, for the impurities at the tetrahedral site the shift is towards lower ones. This no doubt is related to the different geometries in both configurations: at the BC site the impurity is in a much more confined environment, with a strongly directional character (along the bond), while at the T site the impurity is less constrained.

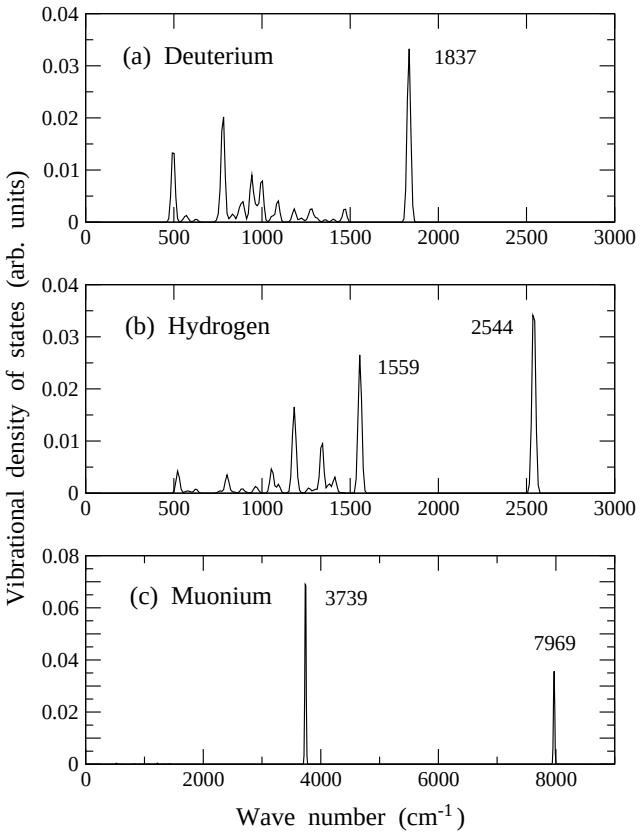

FIG. 7: Vibrational density of states for impurities at a BC site and $T = 300$ K, as derived from a linear-response analysis of PIMD results. Each panel corresponds to an impurity: (a) deuterium, (b) hydrogen, (c) muonium. Labels indicate wave numbers in cm^{-1}. For clarity, discrete modes are presented with a Gaussian profile with a standard deviation of 10 cm^{-1}. Note the different horizontal scale in panel (c).

C. Defect levels in the electronic gap

The DF-TB method employed here allows us to study the influence of zero-point motion on the one-electron levels. For a classical hydrogen-like impurity at a BC site, we find a defect level located in the electronic gap 2.61 eV above the top of the valence band. This result is close to the donor level found by Goss *et al.* from local-density-functional calculations.[16] Also, Saada *et al.* found a defect level at $\sim$ 0.5 eV above the middle of the energy gap for the minimum-energy configuration, which in their case corresponded to the impurity on off-BC sites.[14]

Defect levels associated to the presence of the impurity in the crystal are expected to change as a consequence of electron-phonon interaction. In fact, effects of this kind of interactions on the electronic structure have been experimentally investigated by measuring the temperature dependence of the optical spectra of solids.[46] These effects appear even at low T, due to zero-point motion, and can be large in some cases. For example, in diamond the direct electronic gap (at the Γ point) is reduced by about 0.6 eV with respect to that calculated when zero-point vibrations are neglected.[46] Such studies have been complemented in some cases by observing the dependence of the spectra on isotopic mass, whenever different stable isotopes are available.[47,48]

Similar effects of quantum atomic vibrations should also appear in the defect levels induced by the hydrogenic

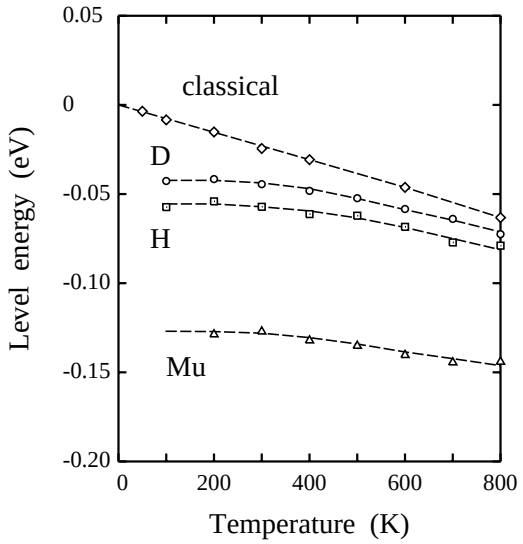

FIG. 8: Temperature dependence of the defect-level energy for deuterium (circles), hydrogen (squares), and muonium (triangles) at a bond center. For comparison, we also present results for a classical simulation (diamonds). The zero of energy corresponds to the level of a classical impurity at $T = 0$. Error bars are on the order of the symbol size. Dashed lines are guides to the eye.

impurities studied here. Shown in Fig. 8 is the temperature dependence of the defect level energy for H, D, and Mu at a BC site in diamond, as derived from our PIMD simulations. For comparison, we also present the energy level E_I derived from classical MD simulations. In this Figure, the zero of energy corresponds to the classical limit at $T = 0$. The most remarkable fact that one observes in this plot is an appreciable shift of the energy level as the impurity mass changes. In particular, for the impurity at the BC site, the level goes down as the mass is lowered. At 300 K we find a decrease in E_I of 13 meV when passing from D to H, and a further decrease of 70 meV when comparing muonium with deuterium. We note also that the level in the case of deuterium is 20 meV lower than that corresponding to a classical impurity (limit of infinite mass) at 300 K. In all cases, the statistical error due to finite sampling of the canonical ensemble is of about 2 meV.

For a given impurity, the defect level goes down as the temperature is raised. In fact, for H and D we find a decrease in the level energy of about 30 meV when T is increased from 100 to 800 K. For muonium, this temperature-induced change amounts to about 20 meV. For the classical impurity this level shift is more important, resulting to be 63 meV.

The position of the defect level for the different impurities at 300 K is given in Table II, where we also present the energy of the level for impurities at the tetrahedral T site. In this case, the classical result at 300 K is found to be 0.58 eV above the defect level for the impurity at a BC site.

For hydrogenic atoms at site T, the level goes up as the impurity mass is lowered, contrary to the case of the bond-center configuration. Also, the level for the T configuration is more sensitive to the impurity mass, since it changes by 0.47 eV from a classical impurity to muonium, vs a decrease of 0.10 eV for the BC configuration.

We note that, while the absolute position of the defect level can depend on the model employed, its relative change induced by temperature and isotopic mass is expected to be quite reliable, because in our analysis both electronic and nuclear dynamics are treated at the level of quantum mechanics, which permits a more realistic description of the electron-phonon interaction in this system.

IV. DISCUSSION

In Sec. III we have presented results of our PIMD simulations for H, D, and Mu in diamond. The main advantage of this kind of simulations is the possibility of calculating defect energies at finite temperatures, with the inclusion of a full quantization of host-atom motions, which are not easy to be accounted for in fixed-lattice calculations. Isotope effects can be readily explored, since the impurity mass appears as an input parameter in the calculations. This includes the consideration of zero-point motion, which together with anharmonicity causes appreciable non-trivial effects. Our results indicate that hydrogenic impurities at the bond-center site cannot be accurately described as a particle moving in a harmonic potential. Even if anharmonicities of the interatomic potential are taken into account, a single-particle approximation does not give reliable results for the impurity complex at finite temperatures. It is then necessary to treat the defect as a many-body problem with anharmonic interactions.

The most prominent feature in the VDOS of the hydrogenic impurities at a BC site is a peak corresponding to the stretching vibration, with a frequency $\omega_{\|}$ higher than the lattice vibrations. This stretching mode is infrared-active, but to our knowledge has not been detected yet. On the theoretical side, there are not many calculations in the literature predicting the frequency of this mode. Goss *et al.*[16] employed an HA from local-density-functional calculations and found for hydrogen at a BC site (in the neutral charge state) a stretching frequency $\omega_{\|} = 2919$ cm^{-1}, somewhat higher than our result using LR calculations ($\omega_{\|,LR} = 2544$ cm^{-1}).

From PIMD simulations we have calculated in Sec. III.A the defect energy $\Delta E_{\rm v}$ for the different hydrogenic impurities. Also, by using the LR procedure we have obtained an approach to the vibrational frequencies of the impurities, which is more realistic than a pure harmonic approximation. These frequencies can now be used to estimate a zero-point energy for the impurities in diamond. In the case of muonium, the modes are almost totally localized on the impurity, and the zero-point vi-

brational energy of the defect is well approximated by $\Delta E^0_{\mathrm{v},LR} = \hbar(\omega_{\perp,LR} + \omega_{\parallel,LR}/2)$. This gives $\Delta E^0_{\mathrm{v},LR} =$ 0.96 eV, close to the ground state energy of the defect presented in Fig. 1 (0.99 ± 0.01 eV). Using the frequencies $\omega_{\perp,HA}$ and $\omega_{\parallel,HA}$ derived from the HA, one finds $\Delta E^0_{\mathrm{v},HA} = 0.57$ eV, much lower than that obtained directly from PIMD simulations. Note that we have used here an expression for E_0 which is only rigorously valid for harmonic oscillators, but it nevertheless gives a good approximation to the zero-point energy of the defect when one introduces the frequencies derived from the LR method. In this sense, these LR frequencies may be considered as renormalized harmonic frequencies, which incorporate in a nonperturbative way anharmonicities of the interatomic interactions, as seen by the atoms in their quantum motion.

The zero-point energy of the defect requires a comment in the sense that, in the case of muonium, it could help to cross the adiabatic barrier for impurity diffusion. Nevertheless, we find that muonium is confined in the BC region, especially at low temperatures. Impurity migration to other regions of the crystal requires important relaxations of the neighboring C atoms, which are not probable at low temperatures. This picture is similar to that described in the literature as "opening of a door",[49] which favors impurity diffusion.

An analysis of hydrogen diffusion in diamond is out of the scope of this paper. As noted above, actual diffusion coefficients are not directly accessible with the kind of MD simulations employed here, since the time scale in the simulations is not readily connected to the real one. In connection with this, PIMD simulations can be applied to study quantum diffusion (including tunneling) of hydrogen in pure and doped diamond, by calculating free-energy barriers in a way similar to that employed earlier to study H diffusion in metals[22] and semiconductors.[50] Even though the rate of H tunneling in diamond is not expected to be high at low T, due to the large lattice relaxation associated to the impurity on a BC site, thermally activated tunneling may be possible, as observed for hydrogen in silicon.[50] This point will require further research.

Theoretical techniques to calculate the electronic band structure of solids have been improving their precision for many years. For various purposes, the accuracy currently achieved by these methods is excellent, when comparing their predictions with experimental data. However, zero-point motion is a significant factor limiting the accuracy of state-of-the-art techniques to predict energy bands. The same happens for defect levels caused by impurities in solids, since their energy may change appreciably as the impurity mass is varied. This effect has been illustrated here by shifts in the energy of the levels due to hydrogenic impurities in BC or T sites in diamond. For muonium at the T site, we have found a level shift of 0.47 eV (upwards), on the order of the renormalization of the diamond gap due to zero-point motion (~ 0.6 eV). For the BC site, the corresponding shift for Mu was 0.10 eV and for H we found 0.03 eV (both downwards). Thus the magnitude and direction of these shifts depend markedly on the mass and position of the impurity in the solid. This behavior can be rationalized by considering the results of perturbation theory for the electron-phonon interaction in the limiting case of a harmonic oscillator.[46,48] The shift of an electronic level is expected to be proportional to the square of the mode amplitude, i.e., proportional to $m^{-1/2}$ in the low-temperature limit and to T at high temperatures. The extrapolation to zero temperature of the defect levels for D, H, and Mu at a BC site (see Fig. 8) gives shifts scaling as $0.72 : 1 : 2.24$, to be compared to the ratio $0.71 : 1 : 2.97$ expected for a harmonic impurity. The energy shift for Mu deviates appreciably from the harmonic expectation, as a consequence of the larger anharmonicity of this impurity center.

In summary, the PIMD method has turned out to be well-suited to study finite-temperature equilibrium properties of light impurities in diamond. This has allowed us to notice the importance of anharmonicity in order to give a realistic description of the properties of these point defects. This anharmonicity shows up in the vibrational modes of the impurities, causing important shifts respect to the harmonic expectancy. Also, zero-point motion introduces an appreciable shift in the defect levels, which depends on the impurity mass. This type of analysis offers a promising way for studying other challenging effects of light impurities in diamond, such as quantum diffusion.

Acknowledgments

The calculations presented here were performed at the Barcelona Supercomputing Center (BSC-CNS). This work was supported by CICYT (Spain) through Grant No. BFM2003-03372-C03-03. ERH thanks DURSI (regional government of Catalonia) for funding through project 2005SGR683.

[1] S. J. Pearton, J. W. Corbett, and M. Stavola, *Hydrogen in Crystalline Semiconductors* (Springer, Berlin, 1992).
[2] S. K. Estreicher, Mater. Sci. Eng. **R14**, 319 (1995).
[3] Y. V. Gorelkinskii and N. N. Nevinnyi, Physica B **170**, 155 (1991).
[4] B. B. Nielsen, K. B. Nielsen, and J. R. Byergen, Mater. Sci. Forum **143-147**, 909 (1994).
[5] C. G. Van de Walle, P. J. H. Denteneer, Y. Bar-Yam, and S. T. Pantelides, Phys. Rev. B **39**, 10791 (1989).
[6] E. Holzschuh, W. Kundig, P. F. Meier, B. D. Patterson, J. P. F. Sellschop, M. C. Stemmet, and H. Appel, Phys. Rev. A **25**, 1272 (1982).

[7] T. L. Estle, S. Estreicher, and D. S. Marynick, Phys. Rev. Lett. **58**, 1547 (1987).
[8] R. Zeisel, C. E. Nebel, and M. Stutzmann, Appl. Phys. Lett. **74**, 1875 (1999).
[9] L. G. Wang and A. Zunger, Phys. Rev. B **66**, 161202 (2002).
[10] T. Miyazaki, H. Okushi, and T. Uda, Phys. Rev. Lett. **88**, 066402 (2002).
[11] J. P. Goss, P. R. Briddon, S. J. Sque, and R. Jones, Phys. Rev. B **69**, 165215 (2004).
[12] E. B. Lombardi, A. Mainwood, and K. Osuch, Phys. Rev. B **70**, 205201 (2004).
[13] S. J. Sque, R. Jones, J. P. Goss, and P. R. Briddon, Phys. Rev. Lett. **92**, 017402 (2004).
[14] D. Saada, J. Adler, and R. Kalish, Phys. Rev. B **61**, 10711 (2000).
[15] J. P. Goss, J. Phys.: Condens. Matter **15**, R551 (2003).
[16] J. P. Goss, R. Jones, M. I. Heggie, C. P. Ewels, P. R. Briddon, and S. Öberg, Phys. Rev. B **65**, 115207 (2002).
[17] A. Kerridge, A. H. Harker, and A. M. Stoneham, J. Phys.: Condens. Matter **16**, 8743 (2004).
[18] M. J. Shaw, P. R. Briddon, J. P. Goss, M. J. Rayson, A. Kerridge, A. H. Harker, and A. M. Stoneham, Phys. Rev. Lett. **95**, 105502 (2005).
[19] F. Buda, G. L. Chiarotti, R. Car, and M. Parrinello, Phys. Rev. B **44**, R5908 (1991).
[20] G. Panzarini and L. Colombo, Phys. Rev. Lett. **73**, 1636 (1994).
[21] S. Bédard and L. J. Lewis, Phys. Rev. B **61**, 9895 (2000).
[22] M. J. Gillan, Phil. Mag. A **58**, 257 (1988).
[23] D. M. Ceperley, Rev. Mod. Phys. **67**, 279 (1995).
[24] T. R. Mattsson and G. Wahnström, Phys. Rev. B **51**, 1885 (1995).
[25] R. Ramírez and C. P. Herrero, Phys. Rev. Lett. **73**, 126 (1994).
[26] C. P. Herrero and R. Ramírez, Phys. Rev. B **51**, 16761 (1995).
[27] T. Miyake, T. Ogitsu, and S. Tsuneyuki, Phys. Rev. Lett. **81**, 1873 (1998).
[28] R. P. Feynman, *Statistical Mechanics* (Addison-Wesley, New York, 1972).
[29] H. Kleinert, *Path Integrals in Quantum Mechanics, Statistics and Polymer Physics* (World Scientific, Singapore, 1990).
[30] G. J. Martyna, M. E. Tuckerman, D. J. Tobias, and M. L. Klein, Mol. Phys. **87**, 1117 (1996).
[31] M. E. Tuckerman, in *Quantum Simulations of Complex Many–Body Systems: From Theory to Algorithms*, edited by J. Grotendorst, D. Marx, and A. Muramatsu (NIC, FZ Jülich, 2002), p. 269.
[32] D. Porezag, T. Frauenheim, T. Köhler, G. Seifert, and R. Kaschner, Phys. Rev. B **51**, 12947 (1995).
[33] C. M. Goringe, D. R. Bowler, and E. Hernández, Rep. Prog. Phys. **60**, 1447 (1997).
[34] B. G. Johnson, P. M. W. Gill, and J. A. Pople, J. Chem. Phys. **98**, 5612 (1993).
[35] T. López-Ciudad, R. Ramírez, J. Schulte, and M. C. Böhm, J. Chem. Phys. **119**, 4328 (2003).
[36] M. C. Böhm, J. Schulte, E. Hernández, and R. Ramírez, Chem. Phys. **264**, 371 (2001).
[37] H. J. Monkhorst and J. D. Pack, Phys. Rev. B **13**, 5188 (1976).
[38] B. J. Skinner, Am. Mineral. **42**, 39 (1957).
[39] M. E. Tuckerman and A. Hughes, in *Classical and Quantum Dynamics in Condensed Phase Simulations*, edited by B. J. Berne and D. F. Coker (Word Scientific, New Jersey, 1998), p. 311.
[40] R. Ramírez and T. López-Ciudad, J. Chem. Phys. **115**, 103 (2001).
[41] R. Ramírez and T. López-Ciudad, in *Quantum Simulations of Complex Many–Body Systems: From Theory to Algorithms*, edited by J. Grotendorst, D. Marx, and A. Muramatsu (NIC, FZ Jülich, 2002), pp. 325–375; for downloads and audio–visual Lecture Notes see `www.theochem.rub.de/go/cprev.html`.
[42] R. Ramírez and C. P. Herrero, Phys. Rev. B **72**, 024303 (2005).
[43] M. Kaukonen, J. Perajoki, R. M. Nieminen, G. Jungnickel, and T. Frauenheim, Phys. Rev. B **61**, 980 (2000).
[44] B. D. Patterson, Rev. Mod. Phys. **60**, 69 (1988).
[45] M. J. Frisch *et al.*, *Computer code GAUSSIAN 98* (Gaussian Inc., Pittsburg, PA, 2001).
[46] M. Cardona, Solid State Commun. **133**, 3 (2005).
[47] S. Zollner, M. Cardona, and S. Gopalan, Phys. Rev. B **45**, 3376 (1992).
[48] M. Cardona and M. L. W. Thewalt, Rev. Mod. Phys. **77**, 1173 (2005).
[49] D. E. Boucher and G. G. DeLeo, Phys. Rev. B **50**, 5247 (1994).
[50] C. P. Herrero, Phys. Rev. B **55**, 9235 (1997).